

## Studies on Tetragonal Lysozyme Crystal Growth Rates

BY ELIZABETH FORSYTHE

*Universities Space Research Association, Huntsville, AL 35806, USA*

FELECIA EWING

*Science and Technology Corporation, Madison, AL 35758, USA*

AND MARC PUSEY\*

*NASA/MSFC, Space Science Laboratory, Biophysics ES 76, Huntsville, AL 35812, USA*

(Received 10 September 1993; accepted 26 November 1993)

### Abstract

A computer-controlled apparatus able to simultaneously follow the face growth rate of up to 40 crystals was developed. This apparatus was used to investigate the effects of solution pH on the (110) and (101) face growth rates of tetragonal lysozyme. Growth rates were measured at pH 4.0, 4.4, 4.8 and 5.2, in 0.1 M sodium acetate buffer with 5% NaCl, 295 K. Initial crystal sizes ranged from 10 to 40  $\mu\text{m}$ . Plots of log supersaturation ratio (either  $C/C_{\text{sat}}$  or  $C/C_{\text{sat}} - 1$ ) versus log(growth rate) are not linear, typically having a slope of  $\sim 8$  at the lowest growth rates determined ( $10^{-6} \mu\text{m s}^{-1}$ ), which falls off to a slope of  $\sim 2$  at the highest growth rates ( $10^{-2} \mu\text{m s}^{-1}$ ) measured. Ratios of  $C/C_{\text{sat}}$  ranged from 4 to  $>20$ . The data show that lower solubility solutions require higher supersaturation ratios for equivalent growth rates. Data for the growth rate of the (101) face at pH 4.0 were widely scattered, especially at lower supersaturation ratios. Time-lapse video of crystals at low supersaturations shows that initially only the (110) faces grow, leaving 'notches' at the (110)–(110) corners. These corners then fill in and macro-steps appear on the (101) faces which rapidly move inward in the form of an octagon, restoring the crystal to a 'normal' appearance. This phenomenon has been observed for tetragonal crystals grown in either still or flowing solutions. Flowing solutions at lower supersaturations also gave cases where the corners did not fill in, with the (110) faces continuing to grow out until growth ceased.

### Introduction

Lysozyme crystallizes as regularly shaped tetragonal crystals under a wide range of conditions. The face growth rates (growth rate) of this crystal form of lysozyme have been studied using a variety of tech-

niques (Fiddis, Longman & Calvert, 1979; Durbin & Feher, 1986; Pusey & Naumann, 1986; Pusey, Snyder & Naumann, 1986; Durbin & Carlson, 1992; Monaco & Rosenberger, 1993; Lorber, Skouri, Munch & Giegé, 1993). While the growth conditions and solubilities have not been the same in all these cases, the data uniformly showed high supersaturation levels and a pronounced dependence of the growth rates on the supersaturation ratio. These data have been interpreted in terms of probable growth mechanism, the role of transport versus attachment kinetics, and the origins of growth steps. Recent efforts have concentrated on the role of impurities in the growth process (Lorber *et al.*, 1993; Vekilov, Ataka & Katsura, 1993).

We have recently completed a computer-controlled video microscopy system, able to monitor the growth of up to 40 widely separated crystals simultaneously (Pusey, 1994). The crystal sizes studied ranged from 10 to 40  $\mu\text{m}$ , which reduces possible size and flow effects on the growth process (Pusey, Witherow & Naumann, 1988). This system now gives us experimental access to growth rates to  $\leq 10^{-6} \mu\text{m s}^{-1}$  with experimental run times of 3–5 d, and we are able to collect a detailed data set of growth data over the  $10^{-6}$ – $10^{-2} \mu\text{m s}^{-1}$  range within a period of 2 weeks. This system is currently being used to study the effects of pH, salt (precipitant) concentration and temperature on the crystal growth of tetragonal lysozyme. A previous report has given a survey of our findings on the effects of temperature and salt concentration at pH 4.0 (Forsythe & Pusey, 1993). In this paper, we present our findings on the effects of pH, observations on a pronounced macro-step observed at lower pH, and the possible relevance of the role of impurities to the observed growth data.

### Materials and methods

Commercial hen egg-white lysozyme (Sigma, 3X crystallized, dialyzed and lyophilized) was further

\* To whom correspondence should be addressed.

purified by ion-exchange chromatography prior to use. The protein was dissolved in and dialyzed against 0.1 M sodium phosphate, 1% NaCl, pH 6.4, in 15 g batches. The dialyzed protein was adsorbed onto a weakly acidic cation-exchange column (Amberlite IRC-50, 16–50 mesh, 5 × 30 cm), which was then washed with the equilibrating buffer. The adsorbed lysozyme was eluted with 3.5% NaCl in the same buffer. Solid NaCl was slowly added with stirring to the eluted protein to give a 10% (w/v) final concentration. The solution was kept overnight at 277 K, after which the crystalline precipitate was recovered, dissolved in and extensively dialyzed against 0.1 M NaAc at the pH of the growth experiments. Prior to dialysis the pH of the protein solution was titrated to the desired pH by addition of dilute acetic acid. Lysozyme concentrations were determined by UV absorbance using an  $A(1\%, 281.5 \text{ nm}) = 26.4$  (Aune & Tanford, 1969).

Face growth rate measurements were made using the computer-controlled video microscopy system (Pusey, 1994). Seed crystals were nucleated *in situ* on the observation chamber walls. From 4 to 30 suitably aligned crystals were selected for following during any given experimental run; the number used being greater the lower the supersaturation employed. Growth solution was freshly prepared prior to each run by mixing equal quantities of buffered protein and salt solutions, which were then injected into the observation chamber (Pusey & Naumann, 1986; Pusey, Snyder & Naumann, 1986). All growth rates were obtained in the absence of imposed solution flow. Solubilities were calculated from published data (Cacioppo & Pusey, 1991).

Observation of macro-steps on the (101) faces was accomplished using a time-lapse video microscopy system (Kozelak & McPherson, 1988). A temperature-controlled observation cell was used which consisted of a pair of microscope slides with a spacer between them to define the growth chamber. This assembly was mounted on a thermostat-controlled block, with the temperature maintained by a circulating water bath. The growth chamber was designed to permit the easy introduction of solutions through standard 1/4–28 chromatography fittings, and designed so that the solutions only contacted teflon and glass. Solutions were passed through the growth chamber system using a dual syringe-pump technique previously described (Pusey *et al.*, 1988).

## Results

The commercial egg-white lysozyme used in these studies was re-purified by ion-exchange chromatography followed by recrystallization prior to use. A sodium dodecyl sulfate (SDS) gel electrophoresis of

the reduced protein, showing the results of these procedures, is pictured in Fig. 1. The non-lysozyme protein impurities ran through the cation ion-exchange column, while most of the lysozyme was bound. By precipitating the subsequently eluted lysozyme at 277 K and high salt we both concentrated the protein and performed a recrystallization. Overall lysozyme yields of ~50% were obtained by this procedure.

Fig. 2 shows the data collected for pH 4.4, 4.8 and 5.2 at 5% NaCl, 0.1 M sodium acetate, 295 K. Data collected at pH 4.0 have been presented previously (Forsythe & Pusey, 1993). The log scale is used to show the data over the more than four orders of magnitude growth rate range measured. While a growth rate asymmetry between the (110) and (101) faces was not observed at pH 4.0, it was found in the data collected at higher pH.

Fig. 3 shows a composite of the (110) and (101) growth rate data using a linear supersaturation ratio ( $C/C_{\text{sat}}$ ) scale for the  $x$  axis. The data collected at pH 4.0, 295 K, 5% NaCl (Forsythe & Pusey, 1993), are included in these plots. Only the averaged rates collected at each protein concentration are shown. We had noted previously a progressive shift to the right in this type of plot under conditions which decrease the saturation concentration, such as increasing salt or decreasing temperature (Forsythe & Pusey, 1993). This general trend was found with changing pH in the (110) growth data. The growth rates at pH 5.2 ( $C_{\text{sat}} = 3.02 \text{ mg ml}^{-1}$ ) are considerably greater than those at pH 4.8 ( $C_{\text{sat}} = 2.05 \text{ mg ml}^{-1}$ ), especially at the lower supersaturation ratios. Solubilities at pH 4.0 and 4.4 are 2.17

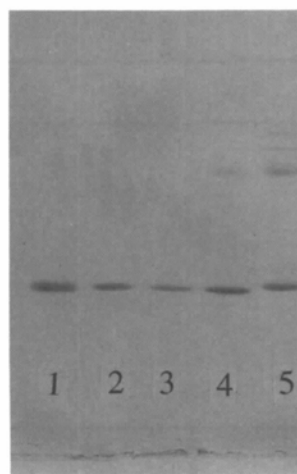


Fig. 1. SDS gel electrophoresis of purified lysozyme. Lanes 1–3, lysozyme bound to, then eluted off of a cation-exchange column. Lane 4, protein which ran through the column without binding. Lane 5, molecular weight standards fibrinogen ( $M_r = 63\,500$ , 56 000 and 47 000) and ribonuclease A ( $M_r = 13\,700$ ).

and  $2.33 \text{ mg ml}^{-1}$ , respectively (Cacioppo & Pusey, 1991). The (101) growth rate data show a similar trend, although the large degree of scatter present in the pH 4.0 data tends to obscure it.

As noted previously for the pH 4.0 growth rate data the (101) growth rates obtained at 295 K and 5% NaCl were widely scattered, and below  $\sim 15 \text{ mg ml}^{-1}$  difficult to obtain (Forsythe & Pusey, 1993). This problem has been most apparent for the data collected at pH 4.0, although it has also been occasionally noted during low supersaturation growth rate experiments at other conditions. The apparently increased prevalence at pH 4.0 may be

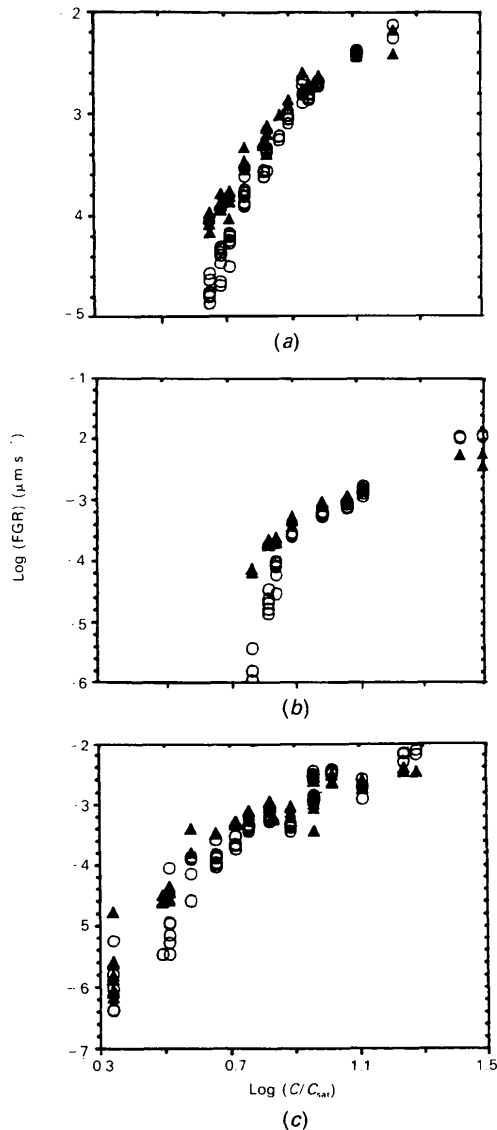


Fig. 2. Log tetragonal lysozyme face growth rates versus log supersaturation ratio, all performed at 295 K, 5% NaCl, and at (a) pH 4.4, (b) pH 4.8 and (c) pH 5.2. Note that different scales are used for the y axes. Symbols:  $\circ$ , (110) faces,  $\blacktriangle$ , (101) faces.

solely due to the greater number of growth rate determinations made there, and thus an increased number of opportunities for observation. Time-lapse video observation of the growing crystals showed that at the initiation of the measurement runs only the (110) faces grew, leaving notches in the non-growing corners. At some point these notches filled in, and gave rise to a pronounced macro-growth step which proceeded to grow across the (101) faces. What triggers the filling-in of the corners, and concomitant macro-step growth on the (101) faces, is not known. This process was documented using time-lapse video microscopy, and a series of frames from a representative event are shown in Fig. 4. Note that the macro-step on the (101) face appears simultaneously on all four corners. Also the macro-growth step is apparently faceted, having eight sides. The progression of this macro-step across the (101) face

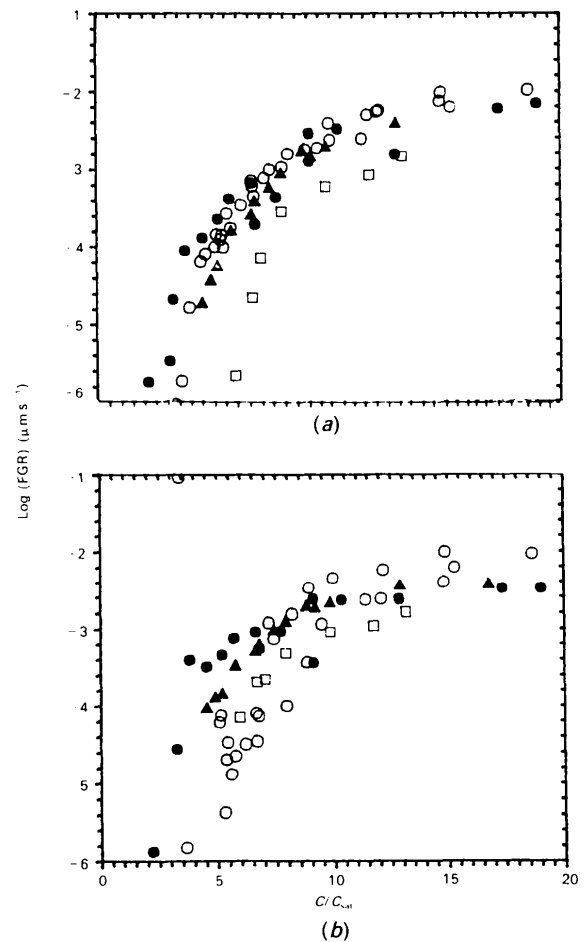


Fig. 3. Comparative effects of pH (saturation concentration) on the (110) (a) and (101) (b) face growth rates of tetragonal lysozyme. The averaged data shown in Fig. 2, plus the pH 4.0, 295 K, 5% NaCl data of Forsythe & Pusey (1993) are shown. Symbols:  $\circ$  pH 4.0,  $\blacktriangle$  pH 4.4,  $\square$  pH 4.8,  $\bullet$  pH 5.2.

was very rapid. From the fourth frame, where the macro-step first appears, to the ninth frame the (110) faces grow  $\sim 2.5 \mu\text{m}$ . The macro-step moves a distance of  $\sim 30 \mu\text{m}$  [one half the distance across the (110) faces] during this same period, having a more than tenfold greater velocity.

During typical pH 4.0 growth rate determinations, sufficient data were collected for (110) rate measurements well before the appearance of the macro-step on the (101) face. However, on several occasions the experimental run was deliberately prolonged and passage of the macro-step could be observed in the data. The results from such a run are shown in Fig. 5. The steep portion of curve *A* indicates movement of the macro-step across the portion of the face being followed by the measuring system. Following the passage of the macro-step the (101) face growth proceeds 'normally', and at a rate greater than that of the (110) face. Also shown on Fig. 5 is curve *B* for the (110) face growth rate data which was obtained concurrently with that for curve *A*. It is apparent from the (110) data that the bulk solute concentration has dropped considerably as shown by a progressive decrease in the measured growth rate. A second (110) growth rate data set, curve *C*, obtained at a slightly lower protein concentration and which is representative of normal (110) growth rate experimental times and data for these conditions, is shown for comparison.

The appearance of the macro-step was also observed under conditions where no solution flow was experimentally imposed upon the system. The data of Fig. 4 were collected under conditions of an imposed flow. While these crystals often showed the appearance of the macro-steps, on other occasions the corners did not 'fill in', and the (110) faces continued to grow outward. In these cases, the faces had progressively smaller cross sections and became more pointed as they grew, with growth itself eventually stopping.

### Discussion

The practical experimental limit for the current apparatus is 3–5 d, which enabled growth rate data collection down to  $10^{-6} \mu\text{m s}^{-1}$ . To acquire growth rates of  $10^{-7} \mu\text{m s}^{-1}$  would require a tenfold longer observation period, leading to serious doubts about the constancy of the protein solution in use. Also, inspection of the plots of log growth rate *versus* log  $C/C_{\text{sat}}$  show that the slopes at low supersaturations are progressively steeper. An order of magnitude decrease in the measurable growth rate range would encompass only a slight decrease in the accessible concentration range.

A general conclusion which can be drawn, based upon this and previous growth rate studies, is that any condition which leads to a reduction in the

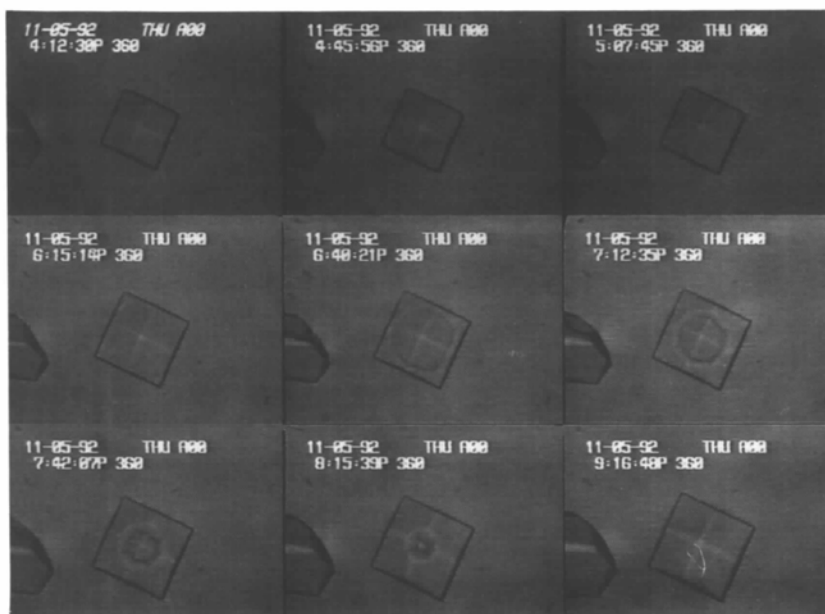


Fig. 4. Effect of low supersaturation growth on (110) and (101) face growth at pH 4.0, 295 K, 5% NaCl, and lysozyme concentration *ca*  $14 \text{ mg ml}^{-1}$ . The field of view in each frame is  $\sim 200 \mu\text{m}$  across. The first frame (upper left corner) is at the initiation of the experiment. The second frame (top center) shows the appearance of notches at the (110)–(110) corners, which are filled in by the third frame (upper right). A macro-step is just appearing at the (110)–(110)–(101) corners by the fourth frame (middle row, far left). A macro-step is also visible on the crystal at the left edge of the field of view.

lysozyme solubility also leads to a requirement for higher supersaturation ratios for a given growth rate. The two extremes of the range of conditions investigated lead to an interesting contrast. At high temperatures and low precipitant concentrations one can have appreciable growth rates ( $\geq 1 \text{ \AA s}^{-1}$ ) at lower supersaturation ranges. At the other extreme, low temperatures and high precipitant concentrations, minimum supersaturation ratios of  $\geq 10$  are required before these minimal growth rates can be obtained. Such ratios are close to the maximum upper limit for growth rates obtained under high solubility conditions.

Growth rates were initially determined at 5% NaCl, pH 4.0. It was noted early during the data acquisition that below  $15 \text{ mg ml}^{-1}$  (101) growth rates became somewhat uncertain, and much more variable than for the (110) face. On occasions when the experimental run length was sufficiently long, (101) growth behaviour as shown in Fig. 5 was observed. Observation of the growing crystals, and time-lapse video microscopy, showed that the cause of the difficulty was initial non-growth of the (101) face, followed by rapid growth due to a macro-step simultaneously originating at the (110)-(110)-(101) corners. This macro-step was observed in both forced-flow and quiescent solution conditions. The onset of the macro-step typically occurred well past the linear portion of the concurrently obtained (110) growth rate data, making it impossible to give an accurate assessment of the lysozyme concentration

in the solution. Forced-flow conditions greatly decreased the lag period prior to the appearance of the macro-step. However, particularly at lower supersaturations, it also often resulted in deformed (110) faces with no corresponding growth (or macro-step) on the (101) faces. As previously observed (Pusey *et al.*, 1988), the solution flow also led to cessation of the growth of the (110) face.

Impurities have recently been invoked to explain the growth data at low supersaturation ranges for tetragonal lysozyme (Lorber *et al.*, 1993; Vekilov *et al.*, 1993). As shown in Fig. 1, and previously demonstrated (Lorber *et al.*, 1993), commercial lysozyme preparations contain impurities which can be removed by chromatographic methods. However, comparison of the data presented in this and previous work with that obtained using less pure material (*i.e.* recrystallized and dialyzed, no chromatographic purification) shows that the overall trends and magnitude of the growth dependence on supersaturation are remarkably similar (Forsythe & Pusey, 1993). The initial non-growth of the (110)-(110) edges under low supersaturation quiescent conditions also suggests impurity effects which are apparently enhanced by the imposition of a flow on the solution.

Given the size of the protein molecule (relative to the solvent), if the impurities are small molecules then they must have specific binding sites to effectively block protein-protein interactions. The binding sites need not be so specific if the impurity molecules are larger. If we assigned the observed low growth totally to impurity effects, then we must conclude that there are pH-, temperature- and precipitant-dependent aspects to impurity binding.

Hen egg-white lysozyme undergoes a phase transition at  $\sim 298 \text{ K}$ , with the crystallographic result that orthorhombic rather than tetragonal crystals are produced. The specific temperature of this transition is a function of the salt concentration and pH (Ewing, Forsythe & Pusey, 1994). Crystal growth studies indicated a time dependence in the phase change orthorhombic  $\rightarrow$  tetragonal: protein solution stored at high temperatures still gave orthorhombic crystals upon cooling then crystallizing (Berthou & Jollès, 1974). Thus, a major impurity may be lysozyme itself, but in the high-temperature or physiological form (Berthou & Jollès, 1974). If so, then addition of a recrystallization step to the chromatographic purification used should reduce the presence of this material. We have initiated experiments to investigate the effect of warmed lysozyme on tetragonal lysozyme crystal growth and test this possibility.

This and previous growth rate data continue to support the concept of tetragonal lysozyme crystal growth proceeding by the addition of pre-formed ordered aggregates from the solution. If the crystal

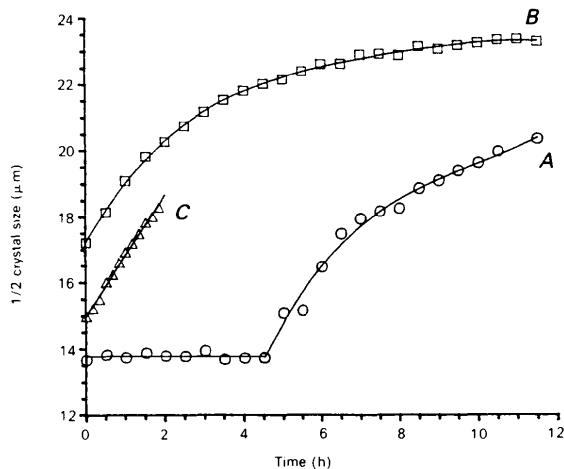


Fig. 5. Appearance of the macro-step during extended quiescent solution face growth rate experiments. Curve A shows the pronounced lag period prior to (101) face growth at low supersaturation. Curve B is the concurrently obtained (110) growth data. Both sets of growth-rate data were obtained at pH 4.0, 295 K, 5% NaCl,  $14.58 \text{ mg ml}^{-1}$  lysozyme concentration. Curve C shows the data from a normal duration growth rate data set collected for the (110) face at  $14.36 \text{ mg ml}^{-1}$  lysozyme concentration.

growth process is a linear function of the concentration of the growth unit, then the current data indicate that at low supersaturations (in fact going to rather high supersaturations in most cases) growth unit concentrations are rather low. If crystal growth is dependent upon the presence of ordered aggregates in the solution, then their concentration would in turn be dependent upon the total soluble lysozyme concentration. Strictly, we cannot speak of an equilibrium constant in a supersaturated solution. However, the species in solution will associate and dissociate at a rate dependent upon their concentration, and the ratio of these two processes can be considered an apparent equilibrium function depending on the solute concentration. This function defines the solution composition which would be obtained were crystal growth blocked. Experimentally, this would define the solutions at lower supersaturations, or at any conditions where the interspecies association–dissociation process proceeds faster than the attachment of the growth units onto the crystal face. Previous studies on tetragonal lysozyme face growth rates have concluded that the rate of growth unit attachment is kinetically, and not transport, limited (Monaco & Rosenberger 1993; Pusey & Naumann, 1986). We postulate then that the growth unit concentration is a function of the apparent equilibria which govern the progression of aggregates, monomer  $\rightarrow$  dimer (...  $\rightarrow$  growth unit). The net effect of lowering the temperature, increasing the salt concentration, or changing the pH, is to lower the overall solubility. These parameters also strongly affect the weak intermolecular interactions characteristic of protein crystals and protein–protein aggregation in general. It is not unreasonable to expect that these parameters will also affect the apparent equilibria (*i.e.* association and dissociation rates)

which govern the formation of aggregates at a given set of conditions, and thus affect the crystal growth rate. What is not known at this point are the comparative rates of association–dissociation *versus* growth unit attachment. However, it may be that some of the effects which are now attributed to impurities are the effects of the solution parameters (pH, temperature, ionic strength) on the aggregation processes which are required to form a non-monomeric growth unit.

#### References

- AUNE, K. C. & TANFORD, C. (1969). *Biochemistry*, **8**, 4579–4590.  
 BERTHOUE, J. & JOLLÈS, P. (1974). *Biochim. Biophys. Acta*, **336**, 222–227.  
 CACIOPPO, E. & PUSEY, M. L. (1991). *J. Cryst. Growth*, **114**, 286–292.  
 DURBIN, S. D. & CARLSON, W. E. (1992). *J. Cryst. Growth*, **122**, 71–79.  
 DURBIN, S. D. & FEHER, G. (1986). *J. Cryst. Growth*, **76**, 583–592.  
 EWING, F., FORSYTHE, E. & PUSEY, M. L. (1994). *Acta Cryst.* **D50**, 424–429.  
 FIDDIS, R. C., LONGMAN, R. A. & CALVERT, P. D. (1979). *Trans. Faraday Soc.* **75**, 2753–2761.  
 FORSYTHE, E. & PUSEY, M. L. (1994). *J. Cryst. Growth*. Submitted.  
 KOSZELAK, S. & MCPHERSON, A. (1988). *J. Cryst. Growth*, **90**, 340–343.  
 LORBER, B., SKOURI, M., MUNCH, J.-P. & GIEGÉ, R. (1993). *J. Cryst. Growth*, **128**, 1203–1211.  
 MONACO, L. A. & ROSENBERGER, F. (1993). *J. Cryst. Growth*, **129**, 465–484.  
 PUSEY, M. L. (1994). *Rev. Sci. Instrum.* **64**, 3121–3125.  
 PUSEY, M. L. & NAUMANN, R. J. (1986). *J. Cryst. Growth*, **76**, 593–599.  
 PUSEY, M. L., SNYDER, R. & NAUMANN, R. J. (1986). *J. Biol. Chem.* **261**, 6524–6529.  
 PUSEY, M. L., WITHEROW, W. & NAUMANN, R. J. (1988). *J. Cryst. Growth*, **90**, 105–111.  
 VEKILOV, P. G., ATAKA, M. & KATSURA, T. (1993). *J. Cryst. Growth*, **130**, 317–320.